Journal of Alloys and Compounds 688 (2016) 958–966

Contents lists available at ScienceDirect

Journal of Alloys and Compounds

journal homepage: http://www.elsevier.com/locate/jalcom

High temperature mechanical properties of as-extruded TiBw/Ti60 composites with ellipsoid network architecture

H.T. Hu [a, b, *], L.J. Huang [b], L. Geng [b, **], J.F. Sun [a], H. Tian [a]

[a] School of Materials Science and Engineering, Heilongjiang University of Science and Technology, P.O. Box 863, Harbin 150022, China
[b] School of Materials Science and Engineering, Harbin Institute of Technology, P.O. Box 433, Harbin 150001, China

ARTICLE INFO

Article history:
Received 11 May 2016
Received in revised form
9 July 2016
Accepted 12 July 2016
Available online 14 July 2016

Keywords:
Titanium matrix composites
As-extruded
High temperature
Mechanical properties

ABSTRACT

In this paper, the as-extruded TiBw/Ti60 composites with ellipsoid network architecture were prepared by powder metallurgy followed by hot extrusion. The high temperature tensile properties of the as-extruded composites were studied in a temperature range of 923–1023 K. The ultimate tensile strength of the as-extruded 5.1 vol.% TiBw/Ti60 composites is increased by 22.0%, 21.2% and 11.4% compared with that of the matrix alloy at 923 K, 973 K and 1023 K, respectively. The excellent improvement in ultimate tensile strength can be mainly attributed to the ellipsoid network microstructure, load-bearing of TiBw and grain refinement. In addition, the elongations of the as-extruded composites are lower than those of the matrix alloy at all temperatures, and decrease with increasing the TiBw content. Fractograph analysis of the as-extruded composites indicates that TiBw fracture dominates the failure of the as-extruded composites at 923–973 K, while the fracture mechanism is predominantly controlled by interfacial debonding at 1023 K.

1. Introduction

Discontinuously reinforced titanium matrix composites (DRTMCs) have attracted extensive attention due to higher specific strength, higher specific modulus, better creep resistance and high temperature durability, which are viewed as the optimal high temperature structural materials in the field of aerospace, military and automotive [1–4]. Especially, TiB whiskers (TiBw) reinforced Ti-alloy matrix composites (TiBw/Ti) prepared by in situ methods are sought-after because of superior properties and low cost [5,6]. Among the various in situ synthesized techniques, powder metallurgy (PM) and vacuum casting technique are considered as the two suitable methods to fabricate the in situ TiBw/Ti composites [7–9]. Compared with the latter, PM route has received more recognition due to its ability for microstructural control, net-shape processing and economic benefit [8]. As is well known, the main aim of developing DRTMCs is to enhance the high temperature properties and service temperature on the basis of titanium alloys [10]. Therefore, one of the critical problems facing the TiBw/Ti composites is how to obtain the higher temperature mechanical properties. As the reinforcement and fabrication method are selected, researchers have already attempted to use near α-Ti alloy as matrix to further improve the high temperature properties of DRTMCs in resent years [11–14].

Near α-Ti alloy belongs to Ti-Al-Sn-Zr-Mo-Si series titanium alloy, such as IMI834, Ti-1100, BT36 and Ti60 alloy [15–18]. It is certainly believed that the higher temperature properties of TiBw/Ti composites can be obtained by selecting near α-Ti alloy as matrix since they possess the highest service temperature of 873 K [19]. Moreover, many experimental results have demonstrated that near α-Ti alloy is effective for the high temperature properties improvement of DRTMCs [11–14]. For example, Xiao et al. selected IMI834 alloy as matrix to fabricate DRTMCs by melting technique, and the composites showed superior high mechanical temperature properties [20]. By employing Ti-6Al-2.5Sn-4Zr-0.7Mo-0.3Si alloy, Zhang et al. fabricated 7.5 vol.% (TiBw + TiC)/Ti-6Al-2.5Sn-4Zr-0.7Mo-0.3Si composites, and the ultimate tensile strength of the composites was increased by 29.1% in relative to the matrix alloy at 923 K [21]. Chandravanshi et al. reported that the TiBw/Ti-1100 composites exhibited higher strength compared with the matrix alloy at 873 K for similar heat treatment conditions [22]. In addition, in our former research [14], the as-sintered TiBw/Ti60

* Corresponding author. School of Materials Science and Engineering, Heilongjiang University of Science and Technology, P.O. Box 863, Harbin 150022, China.
** Corresponding author.
E-mail addresses: haitinghu06@163.com (H.T. Hu), genglingroup@gmail.com (L. Geng).

http://dx.doi.org/10.1016/j.jallcom.2016.07.118
0925-8388/

composites with three-dimensional (3D) network architecture was successfully prepared, and the 5 vol.% TiBw/Ti60 composites exhibited 787 MPa, 625 MPa and 396 MPa at 873 K, 973 K and 1073 K, respectively. It is worth pointing out that the novel network structured TiBw/Ti60 composites exhibits excellent high temperature mechanical properties when compared to the conventional DRTMCs with a homogeneous microstructure [10].

Generally, before most materials are applied to industry, which always need subsequent thermo-mechanical processing such as hot extrusion to further improve the mechanical properties [23]. Although the as-sintered TiBw/Ti60 composites owns superior high temperature mechanical properties, it is expected to obtain much higher temperature mechanical properties of the TiBw/Ti60 composites by hot extrusion. The effort in previous studies on the TiBw/Ti60 composites was mainly concentrated on the high temperature tensile properties under the as-sintered condition and the room temperature tensile properties under the as-extruded condition, respectively [4,14]. However, the high temperature mechanical properties of the as-extruded TiBw/Ti60 composites are still lacking. Therefore, it is meaningful to investigate the high temperature mechanical properties of the as-extruded TiBw/Ti60 composites, which is necessary for the practical application of the kind of composites.

The objective of this investigation is to study the high temperature mechanical properties of the as-extruded TiBw/Ti60 composites at temperatures of 923 K, 973 K and 1023 K, respectively. Additionally, the high temperature fracture mechanisms are also discussed in order to elucidate the influence of temperature on the tensile behavior of the as-extruded composites.

2. Experimental procedures

Based on the our previous published literatures [4,14], large spherical Ti60 powders (180 μm, Ti-5.8Al-4.0Sn-3.4Zr-0.9Ta-0.4Mo-0.4Si-0.37Nb) and fine TiB_2 powders (3 μm) were employed to fabricate the in situ composites with 3D network architecture in the present study. The two kinds of powders were low energy milled with a speed of 200 rpm for 5 h so as to make the fine TiB_2 powders adhere onto the surface of the large Ti60 particles uniformly. Then the milled powders were hot pressed in vacuum (10^{-2} Pa) under the pressure of 20 MPa at 1573 K for 1 h. During the sintering process, TiB whiskers were in situ synthesized between Ti and TiB_2 by the following chemical reaction:

$$Ti + TiB_2 = 2TiB \quad (1)$$

According to the Eq. (1), the 3D network structured TiBw/Ti60 composites with 1.7 vol.%, 3.4 vol.% and 5.1 vol.% of TiBw reinforcement were designed and prepared. Finally, the as-sintered composites billets with dimensions of ϕ60 mm × 40 mm were extruded at 1473 K with an extrusion ratio of 16:1 followed by air cooling. It should be pointed out that the extrusion ratio is the ratio of the cross-sectional area of the as-sintered composites billets to that of the as-extruded bar. Thereby, the diameter of the as-extruded bar was about 15 mm. Additionally, the as-extruded Ti60 alloy was also prepared under identical condition for comparison.

Specimens of microstructure observation were cut from the as-extruded composites. Then the specimens were prepared using conventional techniques of grinding, polishing and etching with Kroll' s solution (5 ml HF, 10 ml HNO_3, 85 ml H_2O) for 7 s. Phase identification was conducted by X-ray diffraction (Riguku D/MAX RB, Cu target). Microstructure characteristics were performed by optical microscopy (OM, Axio Imager A2m), scanning electron microscope (SEM, FEI Quanta 200F) and transmission electron microscope (TEM, Tecnai G2F30). The tensile specimens were cut along the extrusion direction. The gage sections of the specimens are 15 mm × 5 mm × 2 mm. Tensile tests at 923 K, 973 K and 1023 K were carried out on Instron-5569 universal testing machine, driven at constant crosshead speed of 0.5 mm/min. At least three specimens were tested for each composite and average values were reported. To understand the fracture mechanism, the fractured surfaces of the specimens were observed by Hitachi S-4700 SEM.

3. Results and discussion

3.1. Microstructural characteristics

Fig. 1 shows the X-ray diffraction patterns of the as-extruded TiBw/Ti60 composites with different volume fractions of reinforcement. As seen in Fig. 1, the present phases are only Ti and TiB within the as-extruded TiBw/Ti60 composites and no other phases are detected. The phase composition of the as-extruded TiBw/Ti60 composites is the same as that of the as-sintered TiBw/Ti60 composites [14]. This indicates that the phase composition of the TiBw/Ti60 composites does not change after thermo-mechanical processing (TMP). Similar results were also found in other TiBw reinforced titanium matrix composites followed by TMP [9,24].

Fig. 2 shows the OM micrographs of cross sections of the as-extruded Ti60 alloy and 5.1 vol.% TiBw/Ti60 composites. It can be seen from Fig. 2a that the as-extruded Ti60 alloy owns the basket weave microstructure characteristic. The size of α phase in the as-extruded Ti60 alloy is about 10 μm, which is much smaller than that (~300 μm) of the as-sintered Ti60 alloy [14]. This indicates that extrusion deformation can remarkably refine the size of matrix grain. Additionally, it can be carefully observed that the shape of some α laths within α colonies appears to curve with the different degree. It is attributed to the difference of the deformation ability between α phase and β phase during extrusion deformation. As shown in Fig. 2b, the distribution of TiBw displays the quasi-equiaxed network structure around the matrix alloy. The size of the network of the as-extruded TiBw/Ti60 composites can be decreased by extrusion deformation when compared to that of the as-sintered TiBw/Ti60 composites [25].

Fig. 3 shows the microstructure of longitudinal sections of the as-extruded TiBw/Ti60 composites. Compared with the equiaxed network microstructure of the as-sintered 1.7 vol.% TiBw/Ti60 composites [25], the elongated network structure in Fig. 3a can be

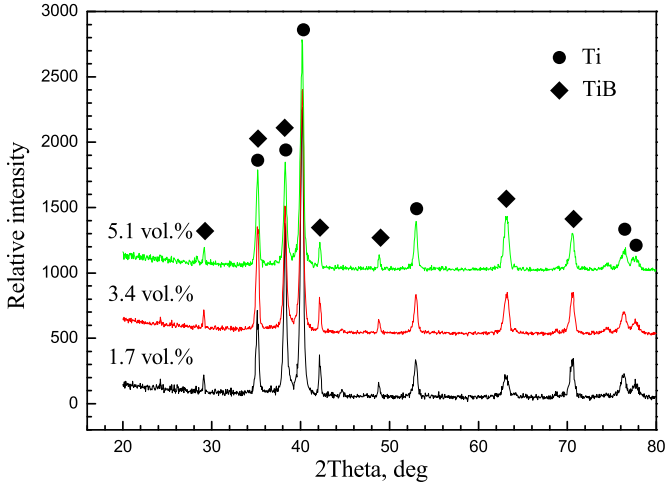

Fig. 1. X-ray diffraction patterns of the as-extruded TiBw/Ti60 composites with different volume fractions of reinforcement.

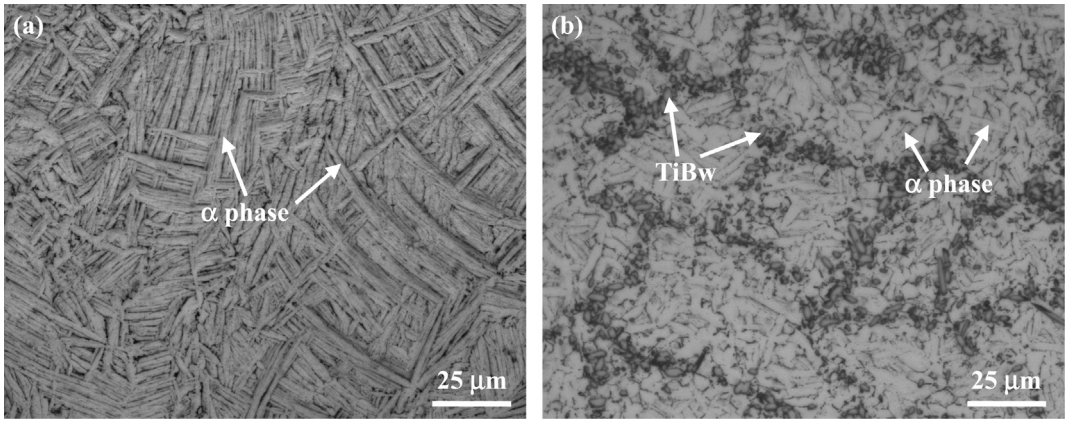

Fig. 2. OM micrographs of cross sections of the as-extruded Ti60 alloy and 5.1 vol.% TiBw/Ti60 composites. (a) Ti60 alloy and (b) 5.1 vol.% TiBw/Ti60 composites.

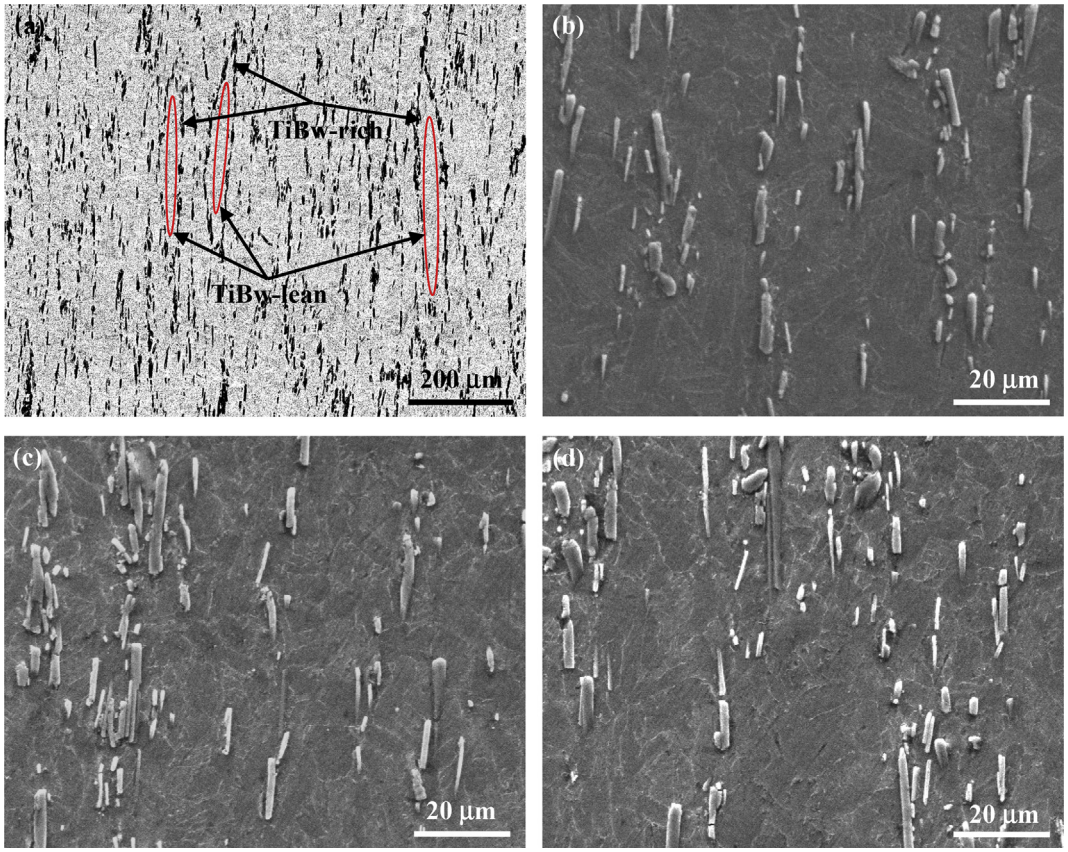

Fig. 3. Microstructure of longitudinal sections of the as-extruded TiBw/Ti60 composites. (a) the BSE micrograph of 1.7 vol.% TiBw/Ti60 composites, (b–d) the SEM micrographs of 1.7 vol.%, 3.4 vol.% and 5.1 vol.% TiBw/Ti60 composites, respectively.

observed after extrusion. In this microstructure, black-colored TiBw reinforcements with ellipsoid distribution exist in the matrix. Internal region of the ellipsoid network microstructure is the TiBw-lean region while the TiBw-rich region is on the boundary. Additionally, it can be seen from Fig. 3b–d that TiBw have aligned along the extrusion direction due to extrusion deformation. The strengthening effect will be improved if the longitudinal direction of TiBw reinforcements is parallel to tensile direction when compared to the random distribution of TiBw [4]. Meanwhile, some fragmented TiBw within the as-extruded composites can be observed leading to the decrease of their aspect ratios. The software Image-Pro Plus analysis shows that the average aspect ratios of the as-extruded 1.7 vol.%, 3.4 vol.% and 5.1 vol.% TiBw/Ti60 composites are 7.0, 6.6 and 6.2, respectively. The result implies that the fracture degree of TiBw of the as-extruded composites with higher TiBw volume fraction becomes more serious during extrusion deformation.

Fig. 4 shows the microstructure of longitudinal sections of the as-extruded Ti60 alloy and 5.1 vol.% TiBw/Ti60 composites at high magnification. It can be observed that the microstructure characteristics in Fig. 4a have no significant change when compared to that of cross section of the as-extruded Ti60 alloy (Fig. 2a).

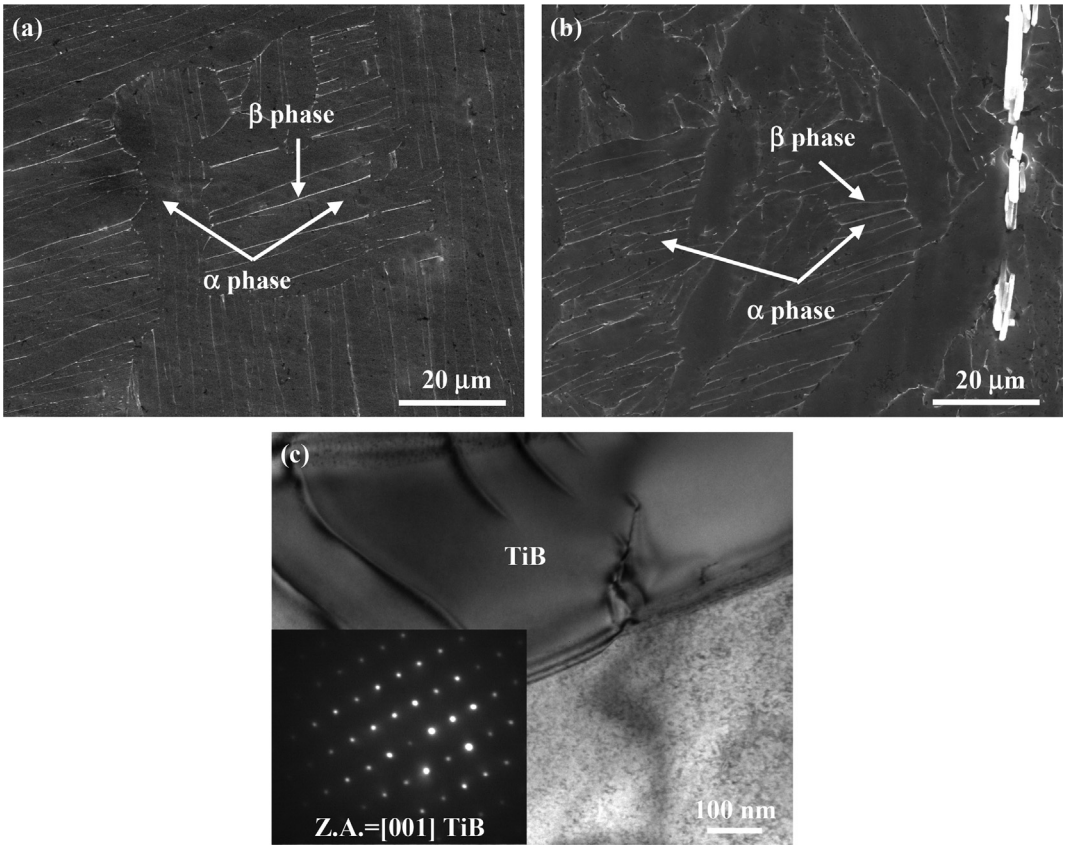

Fig. 4. Microstructure of longitudinal sections of the as-extruded Ti60 alloy and 5.1 vol.% TiBw/Ti60 composites at high magnification. (a) The SEM micrograph of Ti60 alloy, (b) the SEM micrograph of matrix within the as-extruded composites and (c) bright-filed TEM image of TiBw.

However, with regard to the bigger α laths within the as-extruded Ti60 alloy (Fig. 4a), the α laths within the as-extruded composites are finer due to the impeding effect of TiBw on the formation of α laths (Fig. 4b). As is known, the finer α laths within the titanium alloy matrix can contribute to improve the properties of composites than that of composites with bigger α laths [21]. Therefore, it can be deducted that the mechanical properties of the as-extruded composites are better than those of the as-extruded Ti60 alloy. Additionally, the TEM micrograph in Fig. 4c shows that the interface between TiBw and titanium alloy matrix is very clean and no precipitates can be seen, which indicates better bonding force between reinforcement and matrix. Actually, the phenomenon of the strong interfacial bonding between matrix and in situ TiBw is commonly found in the previous studies on TiBw/Ti composites [3,21].

According to the above analysis, the microstructure evolution of the as-sintered TiBw/Ti60 composites in the extrusion direction can be depicted using schematic illustration in Fig. 5. It can be seen from Fig. 5 that four main changes of the microstructure characteristics in the as-sintered composites can be observed after extrusion deformation. Firstly, the original equiaxed network of TiBw has been changed to the ellipsoid distribution of TiBw in the as-extruded composites. Secondly, the randomly distributed TiBw in the as-sintered composites tend to be aligned parallel to the extrusion direction. Thirdly, the matrix microstructure with lamellar α + β structure in the as-sintered composites is developed into transformed β microstructure in the as-extruded composites due to the deformation above the β transus temperature of 1473 K followed by air cooling [4]. Fourthly, the width of TiBw-rich boundary region in the as-extruded composites becomes narrower in relative to that of the as-sintered composites.

3.2. Tensile properties

Fig. 6 shows the ultimate tensile strengths (UTSs) of the as-extruded Ti60 alloy and TiBw/Ti60 composites with different volume fractions of reinforcement in the temperature range of 923–1023 K. It can be obviously seen from Fig. 6 that all the as-extruded composites show much higher UTSs than those of the as-extruded Ti60 alloy at 923 K, 973 K and 1023 K, and the UTSs of the as-extruded composites increase with increasing the reinforcement volume fraction of TiBw. For the as-extruded 5.1 vol.% TiBw/Ti60 composites, the UTS is increased to 783 MPa, 651 MPa and 441 MPa from 642 MPa, 537 MPa and 396 MPa, respectively. That is to say, the UTS can be increased by 22.0%, 21.2% and 11.4% compared with that of the as-extruded Ti60 alloy at 923 K, 973 K and 1023 K, respectively. It is worth noting that the strengthening effect decreases with increasing the testing temperature, especially at 1023 K where it decreases drastically. T he reason for the drastic degradation of the strengthening effect at 1023 K will be discussed later. This phenomenon means that the testing temperature plays an important role on the strengthening effect of TiBw. In addition, the UTS of the as-extruded 5.1 vol.% TiBw/Ti60 composites at 973 K is higher than that of the as-sintered composites with the similar TiBw content [14]. This indicates that the high temperature strength of the as-sintered composites can be improved by extrusion deformation. Meanwhile, compared with the UTSs of 739 MPa, 494 MPa and 356 MPa at 923 K, 973 K and 1023 K of 7.5 vol.% TiBw/near α-Ti composites [9], the present as-extruded composites display an obvious improvement in high temperature strength. Furthermore, the as-extruded composites with 3.4 vol.% and 5.1 vol.% TiBw at 973 K exhibit higher ultimate tensile strength than

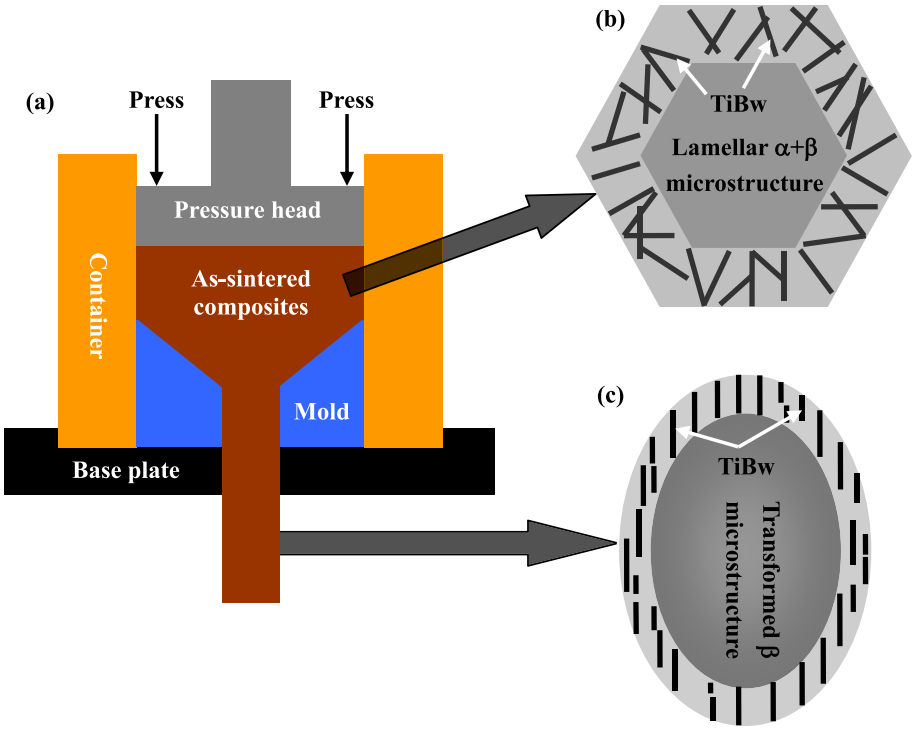

Fig. 5. Schematic illustration of microstructure evolution of as-sintered TiBw/Ti60 composites during extrusion deformation. (a) Experimental set up, (b) the network microstructure unit of as-sintered composites and (c) the network microstructure unit of as-extruded composites.

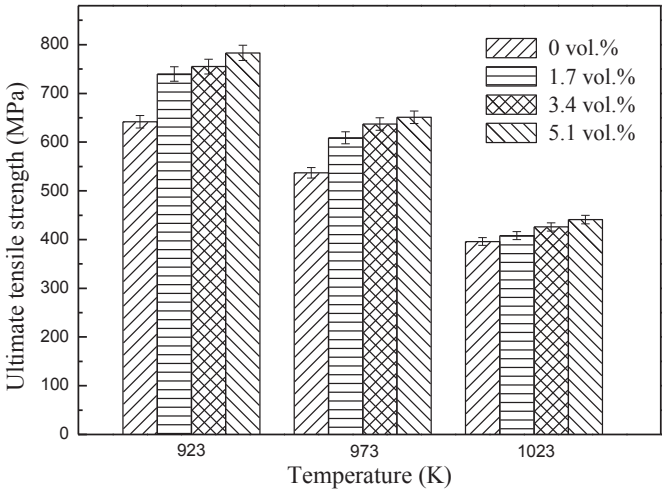

Fig. 6. Ultimate tensile strengths of the as-extruded Ti60 alloy and TiBw/Ti60 composites with different volume fractions of reinforcement in the temperature range of 923–1023 K.

the commercial IMI834 alloy at 873 K [26]. Therefore, the results strongly reveal superior high temperature strength or higher service temperature of the as-extruded TiBw/Ti60 composites with network architecture. It should be pointed out that the UTS of the as-extruded composites is further improved by subsequent heat treatment according to the previous experience [27].

In summary, the increase in UTS at high temperatures of the as-extruded TiBw/Ti60 composites can be attributed to the presence of TiBw. Many studies have also demonstrated that the introduction of TiBw within the composites can effectively strengthen the alloy matrix at high temperatures [3,9,11,27]. Moreover, it is believed that the majority of the strength improvement of TiBw/Ti composites is attributed to load-bearing capacity of TiBw [8,9,28]. As mentioned earlier, TiBw can effectively bear load due to the better interfacial cohesion between the matrix and TiBw. And the TiB whiskers tend to fragment and align along the extrusion direction during extrusion deformation. Therefore, a successful model used by Boehlert et al. [29] is introduced to predict the UTS of the as-extruded composites and explain the strengthening due to TiBw formation in the alloy matrix. The equation used can be expressed as:

$$\sigma_{UTS} = f\sigma_w\xi(\rho_0, m) + (1-f)\sigma_m(\varepsilon_{UTS}) \quad (2)$$

Where f is volume fraction of TiBw, σ_w is TiBw strength, $\xi(\rho_0, m)$ is a numerical factor that depends only on the dimensionless initial TiBw length $\rho_0 = r\sigma_w/L\tau$ and the Weibull modulus (m), $\sigma_m(\varepsilon_{UTS})$ is strength of matrix.

Boehlert et al. [29] have estimated that the TiBw strength (σ_w) is 8 GPa with a Weibull modulus $m = 2$. The r/L values of the as-extruded 1.7 vol.%, 3.4 vol.% and 5.1 vol.% TiBw/Ti60 composites are 0.0714, 0.0758 and 0.1613, respectively, according to their respective average aspect ratios of TiBw mentioned above. Additionally, the $\sigma_m(\varepsilon_{UTS})$ and $\tau = \sigma_m/3^{1/2}$ [29] values of the as-extruded 1.7 vol.%, 3.4 vol.% and 5.1 vol.% TiBw/Ti60 composites can be obtained at the corresponding testing temperature in the present study. Therefore, the UTSs of all the as-extruded TiBw/Ti60 composites at different temperatures can be predicted directly with the above values. Table 1 shows the predicted and measured values. As shown in Table 1, the predicted UTSs of all the as-extruded composites are in reasonable agreement with the experimentally measured values at 923 K and 973 K. The results indicate that load-sharing mechanism dominates the strengthening contribution in the as-extruded TiBw/Ti60 composites at 923 K and 973 K. However, the experimental UTSs of all the as-extruded composites are lower than the predicted values at 1023 K. In fact, the UTS of the as-

Table 1
Predicted UTSs for the as-extruded 1.7 vol.%, 3.4 vol.% and 5.1 vol.% TiBw/Ti60 composites using load-sharing model (Eq. (2)) in the temperature range of 923–1023 K.

As-extruded composites	T (K)	$\rho_0 = (r\sigma_w)/(L\tau)$	ξ (ρ_0, m)	Predicted σ_{UTS} (MPa)	Experimental σ_{UTS} (MPa)
1.7 vol.%	923	1.5417	0.4044	686	740
	973	1.8431	0.3681	578	609
	1023	2.4994	0.3054	431	408
3.4 vol.%	923	1.6351	0.3926	727	755
	973	1.9548	0.3560	616	637
	1023	2.6508	0.2934	462	426
5.1 vol.%	923	1.7406	0.3799	764	783
	973	2.0809	0.3431	650	651
	1023	2.8219	0.2810	491	441

extruded TiBw/Ti60 composites is predicted on the basis of the well-bonded TiBw/matrix interfaces [29]. Thus, the discrepancy between the predicted values and the experimental values at 1023 K can attribute to the decrease in interfacial strength, as also confirmed by Zhang et al. [9]. This implies that load-bearing capacity of TiBw in the as-extruded TiBw/Ti60 composites is limited at 1023 K.

Meanwhile, the grain refinement of matrix caused by TiBw can be conductive to the high temperature tensile strength of the as-extruded TiBw/Ti60 composites, as previously reported by us [14]. The existence of TiBw within the composites can also inhibit grain boundary sliding during the plastic deformation of the composites at high temperatures [30]. Therefore, both the load-sharing of TiBw and grain refinement can contribute to the better high temperature strength of the as-extruded composites.

In addition, the high temperature mechanical properties of the as-extruded TiBw/Ti60 composites were compared with its room temperature mechanical behaviors reported in our previous work [4]. It was found that the improvement in UTS of the as-extruded composites was quite different in relative to the monolithic Ti60 alloy. The strength improvement was more remarkable in the present study when deformed at 923–1023 K than that at room temperature where the largest increment of only 7.5% for composite strength can be obtained. The reason for the superior improvement in UTS can be mainly due to the decrease of local stresses within reinforcements and the improvement of composite ductility at high temperatures, as also confirmed by Zhang et al. [21] and Liu et al. [31].

Fig. 7 shows the elongations of the as-extruded Ti60 alloy and TiBw/Ti60 composites with different volume fractions of reinforcement in the temperature range of 923–1023 K. As shown in Fig. 7, it is evident that the as-extruded composites exhibit much lower elongation than the as-extruded Ti60 alloy due to the existence of TiBw reinforcement at all temperatures. And the elongation increases with increasing the testing temperature and decreases with increasing the reinforcement volume fraction of TiBw. The reason of the variation of the above elongations with testing temperature and TiBw volume fraction (Fig. 7) can be interpreted as the following. On the one hand, the softening of matrix is more and more obvious with enhancing the testing temperature leading to the better plastic deformation ability. On the other hand, the more TiBw volume fraction increases, the bigger the elastic restraint of the deformation ability of the matrix imposed by the TiBw reinforcement becomes.

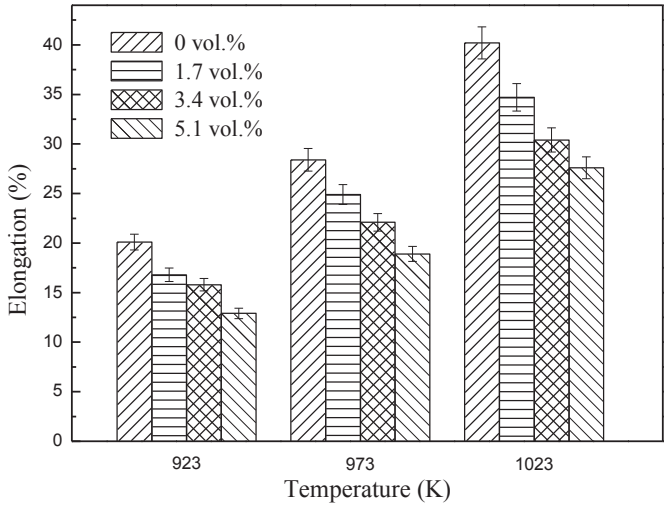

Fig. 7. Elongations of the as-extruded Ti60 alloy and TiBw/Ti60 composites with different volume fractions of reinforcement in the temperature range of 923–1023 K.

3.3. Fracture characteristics

Fig. 8 shows the SEM fractographs of the as-extruded 5.1 vol.% TiBw/Ti60 composites at different temperatures. It can be observed from Fig. 8a that the fracture mechanism of the as-extruded composites at 923 K is typical ductile fracture with lots of dimples in the fracture surface. Moreover, many fractured TiBw are found in center of dimples, revealing a strong interface bonding between the matrix and TiBw. Compared with the fracture features of Fig. 8a, no significant change can be observed in the fracture surface except for more dimples and a few TiBw pull-out in the fracture surface at 973 K (Fig. 8b). However, much larger and deeper dimples can be found in the matrix, which reflect the matrix within the as-extruded composites experiencing larger plastic deformation at 1023 K, as shown in Fig. 8c. And the fractured TiBw substituted by more TiBw pull-out in the fracture surface can be observed. The phenomenon means that the strengthening effect of TiBw within the as-extruded TiBw/Ti60 composites is remarkably decreased and the matrix softening become more serious at 1023 K. The result is consistent with the observed decrease of UTS (Fig. 6) and increase of elongation (Fig. 7) at 1023 K.

In order to better understand the fracture process of the as-extruded composites, the SEM micrographs of the longitudinal sections near the fracture surfaces of the as-extruded 5.1 vol.% TiBw/Ti60 composites at different temperatures are investigated, as shown in Fig. 9. It can be obviously seen from Fig. 9a that TiBw in the longitudinal section fracture are multi-broken and few TiBw can debond with matrix at the interface. This phenomenon demonstrates that the aligned distribution of TiBw can effectively bear load during the tension deformation and exhibit a superior strengthening effect. Combining with the result in Fig. 8a, it can be concluded that the failure mechanism of the as-extruded composites is primarily initiated by the brittle fracture of TiBw reinforcement, followed by ductile failure of the matrix at 923 K. As temperature rises to 973 K, the amount of fractured TiBw (Fig. 9b)

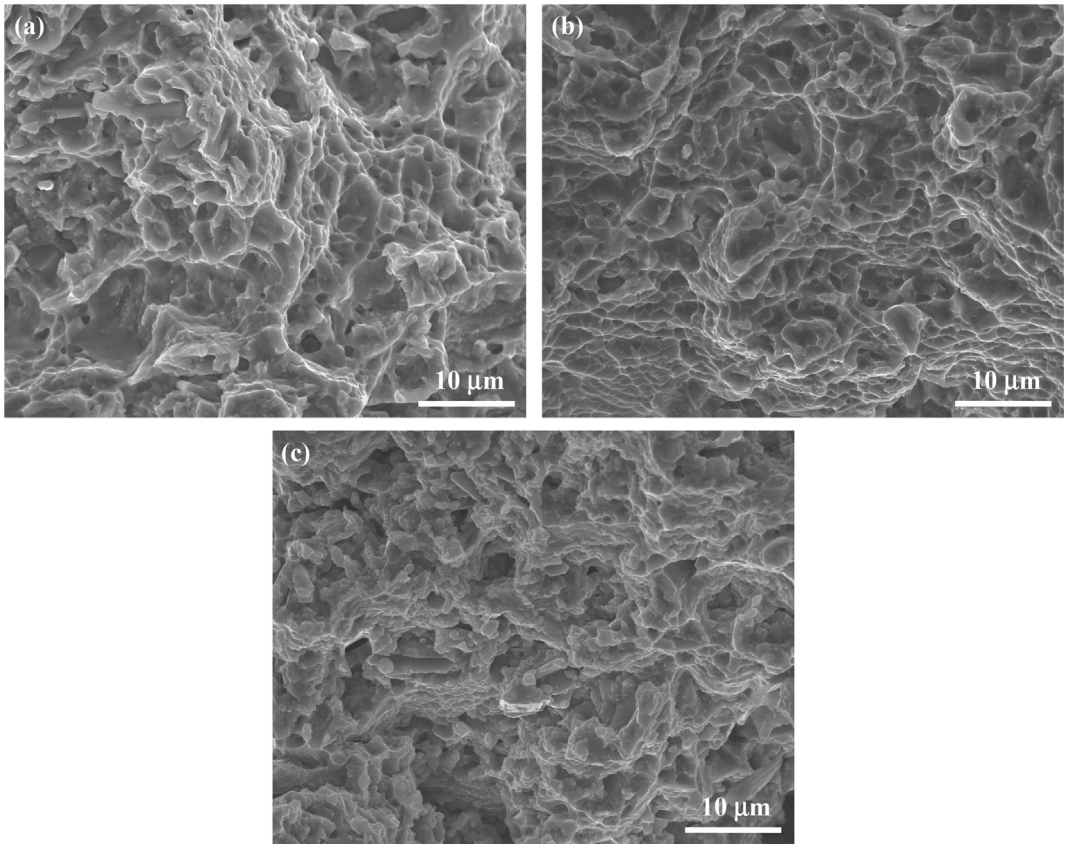

Fig. 8. SEM fractographs of the as-extruded 5.1 vol.% TiBw/Ti60 composites at different temperatures. (a) 923 K, (b) 973 K and (c) 1023 K.

decreases compared with that at 923 K, while the interfacial debonding between TiBw and the matrix generates. Moreover, some voids can be seen not only at the ends of TiBw but also in the matrix except for the sites of the crack of TiBw. However, they do not link each other. It should be pointed out that the amount of fractured TiBw within the as-extruded composites is much bigger than that of TiBw with debonding. The results demonstrate that the fracture of the as-extruded composites is still predominantly controlled by the fracture of the TiBw reinforcement. In other words, the failure mechanism does not change basically with increasing temperature up to 973 K. By contrast with Fig. 9a and b, few fractured TiBw can be seen and the interfacial debonding becomes very common, as shown in Fig. 9c. Generally, interfacial debonding between reinforcements and the matrix is substantially caused by the matrix softening at high temperatures [32]. Together with the variation of elongations with temperature (Fig. 7), it is reasonable to believe that the extent of the matrix softening becomes more greater when the testing temperature is beyond 973 K, which is a good agreement with the analysis of Fig. 8c. Moreover, previous studies have testified that interfacial debonding certainly decreases the load-carrying capacity of TiBw [9,33]. Hence, the incremental UTS of the as-extruded composites at 1023 K is quite limited. This also explains the reason for the drastic degradation of the strengthening effect at 1023 K, as mentioned early in Fig. 6. Additionally, the voids grow longer along the tension direction and link with each other. It is very adverse of the tensile properties of the as-extruded composites since the premature linkage of the longer voids will certainly accelerate the failure of composites. The results show that the interfacial debonding becomes the main failure mechanism of the as-extruded composites at 1023 K. Based on the above analysis, it is easily found that a transition of the failure mechanism of the as-extruded TiBw/Ti60 composites exists at the temperature range investigated. Similar result has been reported in the failure mechanism of TiBw/near α-Ti composites studied in the temperature range of 923–1173 K [9]. This indicates that the fracture behavior of the as-extruded TiBw/Ti60 composites is greatly related to the testing temperature.

Fig. 10 shows the microstructure of the longitudinal section near the fracture surface at low magnification and failure schematic diagram of the as-extruded 5.1 vol.% TiBw/Ti60 composites at 973 K. When loading to the as-extruded TiBw/Ti60 composites, the stronger TiBw-rich network boundary preferentially bears load compared with the softer TiBw-lean matrix region. Then TiBw reinforcements with higher modulus in the ellipsoid network boundary first fracture with the tensile deformation progress. Similar phenomenon was also found in the as-extruded TiBw/TC4 composites [23]. However, the microcracks formed by TiBw breakages can be blunted soon by the matrix around TiBw, as shown in Fig. 10b. This allows the fractured TiBw segments to further bear load and strengthen the composites, eventually leading to the multiple fractures of TiBw, as evidenced by Fig. 9b. Additionally, the microvoids can form by the microcracks coalescence of the adjacent TiBw breakages during tensile deformation. However, the large TiBw-lean matrix region can obstruct the microvoids propagation and further bear strain, which is beneficial to further exploit the strengthening and toughening effects of the network microstructure [34]. Meanwhile, some small cracks within the network boundary are also easily blunted by the soft TiBw-lean region (Fig. 10b), as also confirmed by Fig. 9b. Consequently, the microcracks coalesce to crack when enhanced load is applied. The above phenomena strongly demonstrate that the ellipsoid network microstructure within the as-extruded composites can efficiently

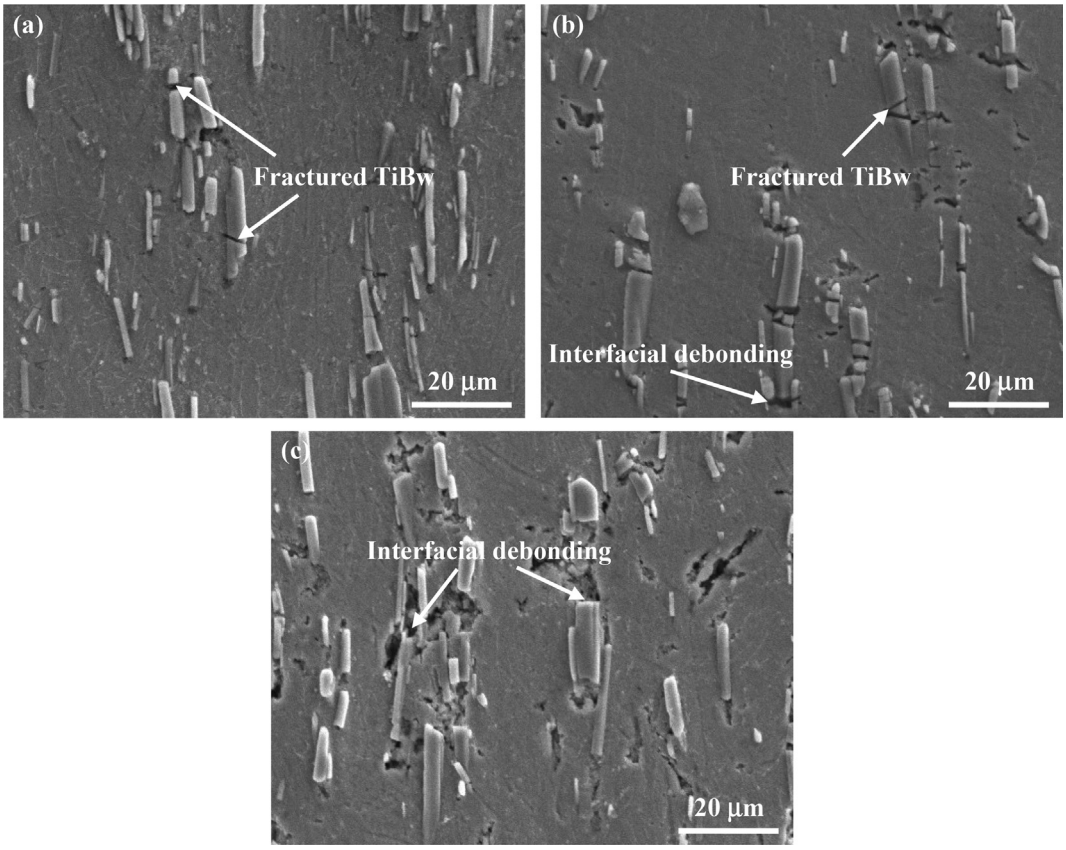

Fig. 9. SEM micrographs of the longitudinal sections near the fracture surfaces of the as-extruded 5.1 vol.% TiBw/Ti60 composites at different temperatures. (a) 923 K, (b) 973 K and (c) 1023 K.

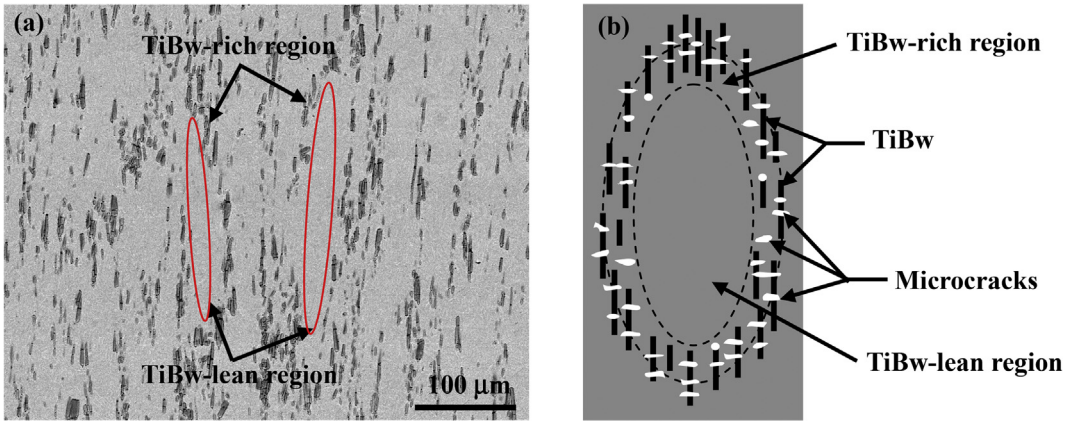

Fig. 10. Microstructure of the longitudinal section near the fracture surface at low magnification and failure schematic diagram of the as-extruded 5.1 vol.% TiBw/Ti60 composites at 973 K. (a) the BSE micrograph of the longitudinal section near the fracture surface and (b) the failure schematic diagram of the as-extruded composites.

utilize the strengthening effect of TiBw reinforcements and the toughening effect of the titanium alloy matrix at high temperatures. It can be also concluded that the mechanical behavior of the as-extruded TiBw/Ti60 composites at high temperatures is mainly controlled by the ellipsoid network microstructure.

4. Conclusions

(1) The ultimate tensile strength of the as-extruded 5.1 vol.% TiBw/Ti60 composites is increased by up to 22.0%, 21.2% and 11.4% in relative to the matrix alloy at 923 K, 973 K and 1023 K, respectively. Moreover, the as-extruded composites with 3.4 vol.% and 5.1 vol.% TiBw at 973 K exhibit higher ultimate tensile strength than the commercial IMI834 alloy at 873 K.

(2) The superior improvement in ultimate tensile strength can be mainly attributed to the ellipsoid network microstructure, load-bearing of TiBw and grain refinement at high temperatures. In addition, the strengthening effect of TiBw decreases with increasing the testing temperatures

substantially due to the reduction of interfacial bonding force and the increment of the extent of the matrix softening.

(3) The failure mechanism of the as-extruded TiBw/Ti60 composites is initiated by the fracture of TiBw followed by ductile damage of the matrix at 923–973 K, while interfacial debonding dominates the fracture mechanism of the as-extruded composites at 1023 K.

Acknowledgements

This work is financially supported by the High Technology Research and Development Program of China (863) under Grant No. 2013AA031202, the National Natural Science Foundation of China (NSFC) under Grant Nos. 51271064 and 51471063 and China Postdoctoral Science Foundation funded project (Grant No. LBH-TZ0506).

References

[1] S.C. Tjong, Y.W. Ma, Mater. Sci. Eng. R 29 (2000) 49–113.
[2] L.J. Huang, L. Geng, H.X. Peng, K. Balasubramaniam, G.S. Wang, Mater. Des. 32 (2011) 3347–3353.
[3] H.B. Feng, Y. Zhou, D.C. Jia, Q.C. Meng, Compos. Sci. Technol. 64 (2004) 2495–2500.
[4] H.T. Hu, L.J. Huang, L. Geng, C. Liu, B. Wang, J. Alloys Compd. 582 (2014) 569–575.
[5] K. Morsi, V.V. Patel, J. Mater. Sci. 42 (2007) 2037–2047.
[6] S. Gorsse, D.B. Miracle, Acta Mater. 51 (2003) 2427–2442.
[7] I. Sen, S. Tamirisakandala, D.B. Miracle, U. Ramamurty, Acta Mater. 55 (2007) 4983–4993.
[8] L.J. Huang, L. Geng, H.X. Peng, B. Kaveendran, Mater. Sci. Eng. A 534 (2012) 688–692.
[9] C.J. Zhang, F.T. Kong, L.J. Xu, E.T. Zhao, S.L. Xiao, Y.Y. Chen, N.J. Deng, W. Ge, G.J. Xu, Mater. Sci. Eng. A 556 (2012) 962–969.
[10] L. Geng, L.J. Huang, Acta Metall. Sin. 27 (2014) 787–797.
[11] L. Xiao, W.J. Lu, J.N. Qin, Y.F. Chen, D. Zhang, M.M. Wang, F. Zhu, B. Ji, Mater. Sci. Eng. A 499 (2009) 500–506.
[12] F.C. Ma, W.J. Lu, J.N. Qin, D. Zhang, Mater. Lett. 60 (2006) 400–405.
[13] W.J. Lu, D. Zhang, X.N. Zhang, R.J. Wu, T. Sakata, H. Mori, Mater. Sci. Eng. A 311 (2001) 142–148.
[14] L.J. Huang, F.Y. Yang, H.T. Hu, X.D. Rong, L. Geng, L.Z. Wu, Mater. Des. 51 (2013) 421–426.
[15] W.J. Jia, W.D. Zeng, Y.G. Zhou, J.R. Liu, Q.J. Wang, Mater. Sci. Eng. A 528 (2011) 4068–4074.
[16] T. Wang, H.Z. Guo, Y.W. Wang, X.N. Peng, Y. Zhao, Z.K. Yao, Mater. Sci. Eng. A 528 (2011) 2370–2379.
[17] N. Singh, V. Singh, Mater. Sci. Eng. A 485 (2008) 130–139.
[18] H. Mishra, P. Ghosal, T.K. Nandy, P.K. Sagar, Mater. Sci. Eng. A 399 (2005) 222–231.
[19] B. Wang, L.J. Huang, B.X. Liu, L. Geng, H.T. Hu, Mater. Sci. Eng. A 627 (2015) 316–325.
[20] L. Xiao, W.J. Lu, Z.F. Yang, J.N. Qin, D. Zhang, M.M. Wang, F. Zhu, B. Ji, Mater. Sci. Eng. A 491 (2008) 192–198.
[21] C.J. Zhang, F.T. Kong, S.L. Xiao, E.T. Zhao, L.J. Xu, Y.Y. Chen, Mater. Sci. Eng. A 548 (2012) 152–160.
[22] V.K. Chandravanshi, R. Sarkar, S.V. Kamat, T.K. Nandy, J. Alloys Compd. 509 (2011) 5506–5514.
[23] L.J. Huang, L. Geng, B. Wang, H.Y. Xu, B. Kaveendran, Composites A 43 (2012) 486–491.
[24] J.X. Li, L.Q. Wang, J.N. Qin, Y.F. Chen, W.J. Lu, D. Zhang, Mater. Sci. Eng. A 527 (2010) 5811–5817.
[25] H.T. Hu, L.J. Huang, L. Geng, B.X. Liu, B. Wang, Corros. Sci. 85 (2014) 7–14.
[26] R. Boyer, E.W. Collings, G. Welsch (Eds.), Materials Properties Handbook, Titanium Alloys, Ohio, 1994, pp. 337–354.
[27] B. Wang, L.J. Huang, L. Geng, X.D. Rong, B.X. Liu, Mater. Des. 85 (2015) 679–686.
[28] K. Prasad, R. Sarkar, S.V. Kamat, T.K. Nandy, J. Alloys Compd. 509 (2011) 7361–7367.
[29] C.J. Boehlert, S. Tamirisakandala, W.A. Curtin, D.B. Miracle, Scr. Mater. 61 (2009) 245–248.
[30] V.K. Chandravanshi, R. Sarkar, P. Ghosal, Metall. Mater. Trans. A 41 (2010) 936–946.
[31] D. Liu, S.Q. Zhang, A. Li, H.M. Wang, J. Alloys Compd. 496 (2010) 189–195.
[32] H.M. Wang, J.Q. Qi, C.M. Zou, D.D. Zhu, Z.J. Wei, Mater. Sci. Eng. A 545 (2012) 209–213.
[33] P.P. Wang, L.Q. Wang, W.J. Lu, J.N. Qin, Y.F. Chen, Z.W. Zhang, D. Zhang, Mater. Sci. Eng. A 527 (2010) 4312–4319.
[34] L.J. Huang, L. Geng, H.X. Peng, Prog. Mater. Sci. 71 (2015) 93–168.